sciendo

Exploration of optoelectronic, nonlinear and charge transport properties of hydroquinoline derivatives by DFT approach

AHMAD IRFAN[1,2,*], ABDULLAH G. AL-SEHEMI[1], AIJAZ RASOOL CHAUDHRY[3], SHABBIR MUHAMMAD[4], RUIFA JIN[5]

[1]Department of Chemistry, Faculty of Science, King Khalid University, Abha 61413, P.O. Box 9004, Saudi Arabia

[2]Research Center for Advanced Materials Science (RCAMS), King Khalid University, Abha 61413, P.O. Box 9004, Saudi Arabia

[3]Deanship of Scientific Research, University of Bisha, Bisha 61922, PO Box 199, Saudi Arabia

[4]Department of Physics, Faculty of Science, King Khalid University, Abha 61413, P.O. Box 9004, Saudi Arabia

[5]College of Chemistry and Chemical Engineering, Chifeng University, Chifeng, China

Present investigation deals with an in depth study of three compounds including 4-(4-chlorophenyl)-8-methyl-2-oxo-1,2,5,6,7,8-hexahydroquinoline-3-carbonitrile (1), 4-(4-bromophenyl)-8-methyl-2-oxo-1,2,3,4,4a,5,6,7-octahydroquinoline-3-carbonitrile (2) and 8-methyl-2-oxo-4-(thiophen-2-yl)-1,2,5,6,7,8-hexahydroquinoline-3-carbonitrile (3) with respect to their structural, electronic, optical and charge transport properties. The ground and excited states geometries were optimized by density functional theory (DFT) and time dependent DFT, respectively. To rationalize the adopted methodology, the calculated geometrical parameters at ground state were compared with the experimental crystal structures. Several quantum chemical insights including the analysis of frontier molecular orbitals (FMOs), total/partial density of states (T/PDOS), molecular electrostatic potentials (MEP), local and global reactivity descriptors revealed that the studied compounds would be efficient multifunctional materials. The absorption wavelengths as well as their major transitions were thoroughly studied at TD-B3LYP/6-31G** level of theory. The smaller hole reorganization energies indicate that all these compounds might show better hole transport tendency. The anionic geometry relaxation of compound 2 is larger than the cationic form which leads to higher electron reorganization energy revealing the reduction of electron charge transport as compared to the hole.

Keywords: *hydroquinoline; electro-optical properties; charge transport properties; reorganization energy; nonlinear optical properties*

1. Introduction

Hydroquinoline derivatives are used as efficient compounds having various applications in optoelectronic devices, semiconductors and pharmaceutical chemistry [1–8]. The compounds of this class are the best biologically active heterocyclic complexes [9, 10] for electro-optical and photonic devices [11]. Moreover, the synthesis of hydroquinoline compounds got significant scientific attention and advancement in the field of novel pharmacophores. Additionally, the improvement of active anticancer drugs is the demand of present era. Previous computational studies of

pyrazolo[3,4-*c*]quinoline derivatives showed reasonable biologically active properties [12]. The hydroquinoline derivatives have been proved excellent antitumor compounds. It has been shown that 8-hydroxyquinoline derivatives demonstrated good cytotoxic activity [13]. Previously, different research groups studied the electronic, optical and QSAR properties of some quinolone derivatives. Bahgat et al. [14] shed light on the effects of chloride, bromide, iodide and nitro substituent on the vibrational frequencies of 8-hydroxyquinoline. Time dependent density functional theory (TDDFT) analysis by Teng et al. revealed that substituents on 8-hydroxyquinoline moiety can improve charge transfer properties [15]. Recently, new styrylquinoline cellular dyes have

*E-mail: irfaahmad@gmail.com

been synthesized and their cytotoxic behavior has been studied in addition to the electronic and spectroscopic properties by TDDFT [16].

Recently, three hydroquinoline derivatives, i.e. 4-(4-chlorophenyl)-8-methyl-2-oxo-1,2,5,6,7,8-hexahydroquinoline-3-carbonitrile (1) [17], 4-(4-bromophenyl)-8-methyl-2-oxo-1,2,3,4,4a,5,6,7-octahydroquinoline-3-carbonitrile (2) [18] and 8-methyl-2-oxo-4-(thiophen-2-yl)-1,2,5,6,7,8-hexahydroquinoline-3-carbonitrile (3) [19] were synthesized (Fig. 1). According to the recent literature review and to the best of our knowledge, these compounds have not been studied computationally with respect to structure-activity relationship (SAR), electro-optical properties, charge transport nature and nonlinear optical properties (NLO). In the present study, we aim to investigate the structural, electro-optical and charge transfer properties of hydroquinoline derivatives (1 – 3). We have studied the SAR, shedding light on the molecular geometries, frontier molecular orbitals (FMOs), excitation energies and absorption spectra as well as their major transitions that involve the FMOs. Furthermore, their total/partial densities of states (T/PDOS), molecular electrostatic potentials (MEP), local and global reactivity descriptors were analyzed. Additionally, to understand the charge transport nature of these compounds, we shed light on the charge transport properties (vertical/adiabatic ionization potentials (IPv/a), vertical/adiabatic electron affinities (EAv/a), hole and electron reorganization energies $(\lambda_{\mathrm{h}}/\lambda_{\mathrm{e}})$). Quantum chemical investigations [20–28] were performed by using DFT and TDDFT.

2. Computational details

Previous studies showed that DFT and TDDFT are good tools to understand the electro-optical properties, charge transport behavior and nature of the charge transport [29–32]. The B3LYP functional is an appropriate choice to reproduce the experimental data for metal containing and metal free small compounds [33–37] and geometrical parameters for transition metal compounds [38]. Sousa et al. [39] investigated the geometrical properties of different compounds and found that B3LYP
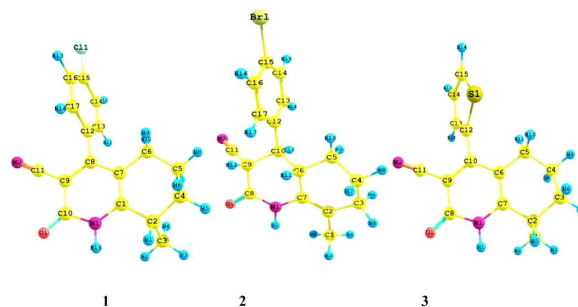
Fig. 1. The structures of hydroquinoline derivatives 4-(4-chlorophenyl)-8-methyl-2-oxo-1,2,5,6,7,8-hexahydroquinoline-3-carbonitrile (1), 4-(4-bromophenyl)-8-methyl-2-oxo-1,2,3,4,4a,5,6,7-octahydroquinoline-3-carbonitrile (2) and 8-methyl-2-oxo-4-(thiophen-2-yl)-1,2,5,6,7,8-hexahydroquinoline-3-carbonitrile (3).

is the best one among the B1B95, B97-2, BP86 and BPW91 functionals. Moreover, B3LYP functional was employed to investigate the photochemical properties of anti-inflammatory drugs [40]. Additionally, the experimental absorption spectra of various molecules have been reproduced well with an average deviation of 0.20 eV [41]. A number of properties of interests for multifunctional compounds have been calculated at B3LYP functional and those were found in reasonable agreement with their respective experimental data [42–44]. Additionally, previous work revealed that the B3LYP/6-31G** level of theory is good to predict the electronic and charge transport properties of sulfur compounds [45]. In the current study, the ground and excited state geometries have been optimized by DFT [46–51] at B3LYP/6-31G** and TDDFT levels of theory which have been proved as effective approaches, respectively [52–54]. The TD-B3LYP/6-31G** level was applied to optimize the first excited state geometries of the studied compounds. The absorption wavelengths were calculated by TDDFT that proved to be an effective method [55].

The reorganization energy (λ) has been used to approximate the ability of charge carriers [56, 57], to be divided into two parts; $\lambda_{\mathrm{rel}}^{(1)}$ and $\lambda_{\mathrm{rel}}^{(2)}$; the geometry relaxation energy from neutral to charged (cation/anion) state is $\lambda_{\mathrm{rel}}^{(1)}$ while geometry

relaxation energy from charged (cation/anion) to neutral state is $\lambda_{\text{rel}}^{(2)}$ [58]:

$$\lambda = \lambda_{rel}^{(1)} + \lambda_{rel}^{(2)} \qquad (1)$$

In the present study, both the parts of λ have been evaluated from the adiabatic potential energy surfaces [59]:

$$\lambda_{rel}^{(1)} = E^1(C) - E^0 \qquad (2)$$

$$\lambda_{rel}^{(2)} = E^1(C)^{+/-} - E^0(C)^{+/-} \qquad (3)$$

The $\lambda(h)$ and $\lambda(e)$ were evaluated as:

$$\lambda(h) = [E^1(C)^+ - E^0(C)^+] + [E^1(C) - E^0(C)] \qquad (4)$$

$$\lambda(e) = [E^1(C)^- - E^0(C)^-] + [E^1(C) - E^0(C)] \qquad (5)$$

where $E^0(C)$ and $E^0(C)^{+/-}$ are the ground state energies of neutral as well as charged (cation/anion) species, respectively; $E^1(C)$ is the neutral molecule energy at the optimized geometry of charged species while $E^1(C)^{+/-}$ is the charged species energy at the geometry of the optimized neutral molecule, respectively. The EAa, EAv, IPa and IPv were evaluated as:

$$EAa = E^0(C) - E^0(C)^- \text{ and } EAv = E^0(C) - E^1(C)^- \qquad (6)$$

$$IPa = E^0(C)^+ - E^0(C) \text{ and } IPv = E^1(C)^+ - E^0(C) \qquad (7)$$

where, $E^0(C)$, $E^0(C)^+$ and $E^0(C)^-$ are the energies of neutral, cation and anion at the ground state, whereas $E^1(C)^+$ and $E^1(C)^-$ represent the energy of charged cation and anion state at the optimized neutral geometry of the molecule, respectively. All these charge transport parameters were computed at B3LYP/6-31G** level of theory.

Mulliken electronegativity (χ) was calculated from the following equation:

$$\chi = (IP + EA)/2 \qquad (8)$$

Hardness (η) can be evaluated by using equation 9:

$$\eta = (IP - EA)/2 \qquad (9)$$

Electrophilicity (ω) can be assessed by using equation 10:

$$\omega = (IP + EA/2)^2/2\eta \qquad (10)$$

Softness (S) can be estimated by using equation 11:

$$S = 1/2\eta \qquad (11)$$

Electrophilicity index (ωi) can be calculated by using equation 12:

$$\omega i = \mu^2/2\eta \qquad (12)$$

Chemical potential (μ) can be evaluated by using equation 13:

$$\mu = -(IP + EA/2) \qquad (13)$$

All these calculations were carried out by implementing the Gaussian 09 package [60].

To determine the total and partial DOS (T/PDOS) at bulk level by considering the boundary conditions, CASTEP module [61] implemented in Materials Studio [62] was used. Here, the exchange and correlation energy/potential have been treated using the Perdew et al. [63] parameterized GGA within DFT. To evaluate the TDOS and PDOS, ultra-soft pseudo-potential has been applied. The cut-off energy in plane wave expansion was assumed as 300 eV, whereas the SCF tolerance for this run was 2×10^{-6} eV/atom.

3. Results and discussion

3.1. Geometries

The ground and excited states geometrical parameters, i.e. bond lengths and bond angles, computed at B3LYP/6-31G** and TD-B3LYP/6-31G** levels of theory, respectively have been collected in Table 1 (atom numbers can be seen in Fig. 1). The calculated ground state geometries

Table 1. Selected optimized bond lengths in angstrom (Å) and bond angles (degree) of ground and first excited states for hydroquinoline derivatives at the B3LYP/6-31G** and TD-B3LYP/6-31G** levels of theory.

Parameters		1^a	2^b	3^c
C1-N1	Neutral	1.366 (1.356)	1.413 (1.407)	1.366 (1.366)
	Excited	1.371	–	1.356
C10-N1	Neutral	1.403 (1.368)	1.369 (1.338)	1.401 (1.370)
	Excited	1.384	–	1.450
C10-O1	Neutral	1.223 (1.241)	1.219 (1.225)	1.223 (1.247)
	Excited	1.260	–	1.223
C11-N2	Ground	1.164 (1.150)	1.160 (1.118)	1.164 (1.148)
	Excited	1.170		1.169
C15-Ht1	Ground	1.757 (1.745)	1.910 (1.901)	–
	Excited	1.758		–
N1-C10-O1	Neutral	120.55 (121.23)	122.11 (122.99)	120.52 (121.57)
	Excited	115.92	–	116.35
C9-C10-O1	Ground	127.05 (118.20)	121.87 (120.46)	126.90 (123.97)
	Excited	126.43	–	129.21
C14-C15-Ht1	Neutral	119.42 (119.05)	119.62 (119.43)	–
	Excited	119.64	–	–

Experimental data in parentheses from the literature: [17][a], [18][b], [19][c]; Ht = Cl/Br

were compared with the experimental crystal structural parameters [17–19].

Additionally, the alterations in the bond lengths and bond angles have been studied from the ground to excited states. The deviation in the bond lengths between the calculated and experimental crystal structures has been observed as follows: the calculated C_{10}–N_1 (C_{11}–N_2) bond lengths have been overestimated: 0.035 (0.014) Å, 0.031 (0.042) Å and 0.031 (0.016) Å for derivatives 1 – 3, respectively. The computed C_{10}–O_1 bond length has been underestimated of 0.018 Å, 0.006 Å and 0.024 Å for 1 – 3, respectively as compared

to the experimental crystal structure data. On other hand, alteration from ground to excited states (for both the calculated geometries) has been perceived as follows: the calculated C_{10}–N_1 bond length has been shortened of 0.019 Å while C_{10}–O_1 bond length has been lengthened of 0.037 Å in 1. The calculated C_{10}–N_1 bond length has been lengthened of 0.051 Å in 3.

The deviation in the bond angles between the calculated and experimental crystal structures has been observed as follows: computed C_9–C_{10}–O_1 bond angles have been overestimated of 8.85°, 1.41° and 2.93° in 1 – 3, respectively. The alteration from ground to excited states has been observed as follows: the calculated N_1–C_{10}–O_1 bond angle has been decreased of 4.63° and 4.17°, while C_9–C_{10}–O_1 bond angle has been increased of 2.31° in 1 and 3, respectively. It is expected that the overestimation or underestimation in the calculated bond lengths/angles as compared to the crystal structural parameters is due to fact that the experimental data have been collected in the packing and solid state whilst the computed data refer to the gas phase. This can be verified as the calculated bond lengths of C–C, C–S, C–Cl and C–Br in the thiophene and phenyl units (which have proper conjugation) are in reasonable agreement with the experimental data. Moreover, the computed bond lengths C–Cl, C–Br, and bond angles C_{14}–C_{15}–C_l and C_{14}–C_{15}–Br have been found in decent agreement with the experimental data.

3.2. Electronic structure and absorption spectra

In Fig. 2, charge density patterns of the highest occupied molecular orbitals (HOMOs) and the lowest unoccupied molecular orbitals (LUMOs) have been depicted. At the ground state, the HOMO and LUMO are distributed on the quinoline (heteroatoms containing side chains) and carbonitrile in 1; in 2, HOMO is distributed at quinoline (heteroatoms containing side chains) while LUMO at phenyl moiety; in 3, HOMO and LUMO are distributed at quinoline (heteroatoms containing side chains) and thiophene. The comprehensive intramolecular charge transport is observed in 2. The

calculated HOMO energies (E_{HOMO}), LUMO energies (E_{LUMO}) and HOMO-LUMO energy gaps (E_g) at B3LYP/6-31G** levels of theory are tabulated in Table 2.

The E_{HOMO} usually increases from 1 to 3. The lowest E_{LUMO} is observed for 3 while the highest for 1. The E_g value has been observed in the order $3 < 1 < 2$. The E_g has been used as kinetic stability indicator of the compound. The higher value of E_g reveals that the studied compound would be thermodynamically more stable.

HOMOs   LUMOs
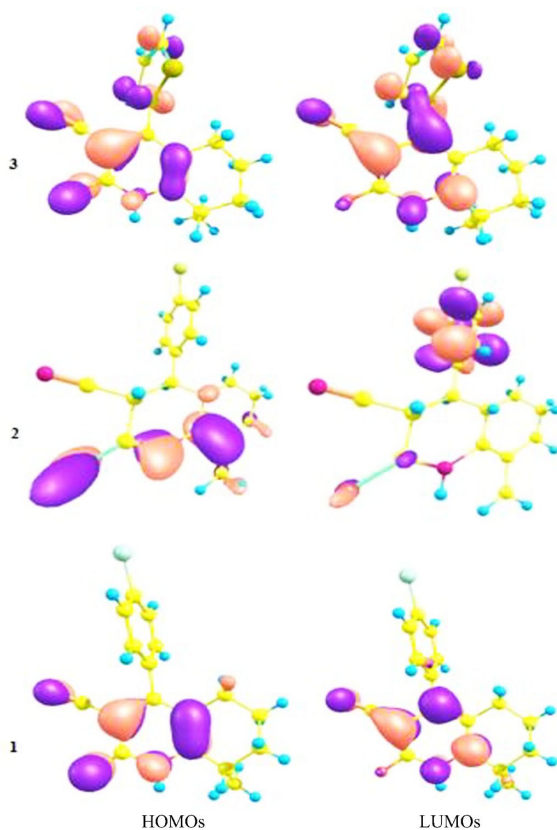
Fig. 2. Distribution patterns of the HOMOs and LUMOs of hydroquinoline derivatives at the ground states.

The calculated absorption wavelengths (λ_a) of $1 - 3$ at TD-B3LYP/6-31G** level of theory have been disclosed in Table 2. The major transition in the absorption spectra has been observed from HOMO to LUMO (H $\rightarrow$ L). The first λ_a has been noted at 328 nm with the oscillator strength of 0.1976 in 1. In 2, the λ_a has been 67 nm blue shifted

as compared to the first absorption wavelength of 1. The oscillator strength is reduced to the 0.0755. In 3, the λ_a has been 14 nm and 81 nm red shifted as compared to the 1 and 2. The oscillator strength of 3 is higher than 2 while less than 1.

3.3. Density of states

For comprehensive understanding of the electronic structures of derivatives ($1 - 3$), we determined their total and partial DOS using GGA/PW91 implemented in CASTEP software program available in Materials Studio within the framework of DFT. The TDOS and PDOS with contributions from C, O, N, Cl, Br and S atoms have been shown in Fig. 1 to Fig. 3 for derivatives $1 - 3$, respectively. In compound 1, the energy band in the deep valence region at the energy regime of -20 eV to -10 eV is defined mostly by the s orbitals of all atoms. While in the energy regime of -18 to -10 eV, the major contribution is from s orbitals of C atoms. The s orbitals of O atoms are contributing from -22 eV to -18 eV, N atoms from -22 eV to -17 eV and Cl from -18 eV to -15 eV. Similarly, the peaks in upper valence bands from -10 eV to 0 eV are due to the p orbitals of C, O, N and Cl atoms. In lower conduction bands, the peaks are due to the p orbitals of C and N atoms only.

For derivative 2, at lower valence bands, the s orbitals of C atoms are contributing in energy range of -39 eV to -9 eV, the s orbital of O atoms has one peak at -35 eV, the s orbitals of N atoms show one peak at -38 eV and one peak at -18 eV and the s orbital of Br atom is taking part mostly at -35 eV and in energy range of -23 eV to -19 eV. The p orbitals of C atoms have major part in the valence bands, O atoms have a minor contribution from p orbitals in valence bands, the p orbitals of N atoms have the major contribution at -38 eV, -28 eV and -23 eV with a minor contribution in the energy range from -20 eV to 0 eV, whereas the p orbitals of Br atom have minor contribution in the energy range of -23 eV to -14 eV and a major contribution of p orbitals has been found in the energy range of -14 eV to 0 eV in the upper valence bands.

For derivative 3 at valence bands, the s orbitals of C atoms have minor contribution in the energy

Table 2. HOMO energies (E_{HOMO}), LUMO energies (E_{LUMO}), and HOMO-LUMO energy gaps (E_g) in [eV] for ground states and calculated absorption wavelengths (λ_a) of hydroquinoline derivatives at the B3LYP/6-31G** and TD-B3LYP/6-31G** level of theories.

Compounds	E_{HOMO}	E_{LUMO}	E_g	f	λ_a [nm]	λ_a [eV]	Transition
1	–6.15	–1.98	4.17	0.1976	328	3.780	H → L
2	–6.09	–0.087	5.22	0.0755	261	4.750	H → L
3	–6.05	–2.05	4.00	0.1455	342	3.625	H → L

range of –33 eV to 0 eV, the s orbitals of O atom have a major contribution at –23 eV, the s orbitals of N atoms are contributing from –32 eV to –30 eV and from –26 eV to –19 eV and the s orbitals of S atom are taking part mostly at –31 eV to –15 eV. The p orbitals of C atoms are contributing mostly in the valence bands in energy range from –31 eV to 0 eV and from 0 eV to 2 eV in conduction bands. The O atom has the contribution from p orbitals in higher valence bands at –9 eV to –2 eV, the p orbitals of N atoms have the minor contribution from –21 eV to –14 eV and the major contribution in upper valence bands from –12 eV to 0 eV with a minor contribution in the energy range from 0 to 2 eV in conduction bands. Whereas the p orbitals of S atom have a minor contribution at –32 eV, −21 eV and in the energy range of –11 eV to –1 eV and the major peak of p orbitals has been found at –2 eV in the upper valence bands, while in conduction bands, S atom is contributing from 0 eV to 2 eV.

3.4. Analysis of molecular electrostatic potential (MEP) surfaces

Molecular electrostatic potential (MEP) surfaces are very beneficial features to investigate the reactivity of a molecule. In the MEPs, the regions with the major negative potential are shown in red color and these regions are favored location for electrophilic attack, whereas the regions with maximum positive potential, indicated with blue color, are ideal sites for nucleophilic attack. The MEP instantaneously shows not only the size and shape of molecule but also the neutral, negative and positive electrostatic potential of the compound as is displayed in Fig. 3. The MEP decreases in the order blue > green > yellow > orange > red, while the red color indicates the strongest repulsion, and the

blue illustrates the sufficient attraction. The lone pair of electronegative atoms is mainly associated with the negative potential regions. It can be seen from the MEP of the derivatives that the negative potential region is on the Cl atoms in derivative 1. The N atoms in all the studied derivatives exhibit the positive electrostatic potential regions whilst the Br atom has intermediate electrostatic potential. In accordance with this, the Cl atom in the derivative 1, indicated by the red color, performs as electrophilic region. Likewise, the blue color denotes the nucleophilic regions and illustrates the regions with electron deficiency. These outcome reveals that the maximum attraction is indicated by N atoms, while the substantial repulsion is shown by Cl atoms.
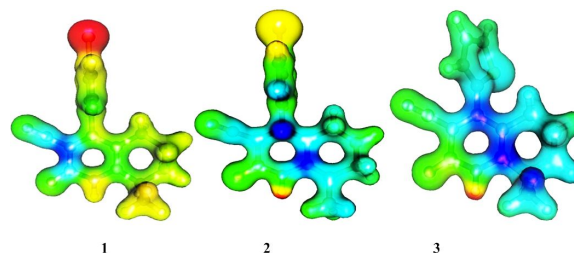
Fig. 3. Molecular electrostatic potential surfaces (MEP) of hydroquinoline derivatives investigated in the presented study.

3.5. Global and local reactivity descriptors

The global reactivity descriptors e.g. electronic chemical potential (μ), electronegativity (χ), hardness (η), softness (S) and electrophilicity index (ωi) calculated at the B3LYP/6-31G** level of theory have been presented in Table 3. The μ describes the escaping affinity of electron from a stable

compound. Actually, the μ of an atom is occasionally believed to be the negative of the atom's electronegativity. The η reveals the resistance to variation in electron distribution which is interconnected with the stability and reactivity of the chemical system. The converse of the η is called S. The ωi represents the energy depression owing to prominent electron movement between acceptor and donor. The values of χ, η, S, and ωi for 1 – 3 derivatives are 3.85 eV, 3.83 eV, 0.13 eV and 1.93 eV; 3.74 eV, 3.74 eV, 0.13 eV and 1.87 eV; and 3.79 eV, 3.76 eV, 0.13 eV and 1.91 eV, respectively. Lower values of η and χ of 2 compared to other counterparts reveal that mentioned compound would be more stable with lower chemical activity.

Table 3. The global reactivity descriptors of 1 – 3 derivatives obtained at B3LYP/6-31G** level of theory.

	1	2	3
χ	3.85	3.74	3.79
η	3.83	3.74	3.76
ω	1.94	1.87	1.91
S	0.13	0.13	0.13
ωi	1.93	1.87	1.91
μ	–3.85	–3.74	–3.79

If the electrons change in a molecule then the local reactivity descriptor e.g. Fukui function points out the favorite regions where a chemical species adjusts their density [64]. On the jth atom site, the condensed or atomic Fukui functions can be defined as:

$$f_j^+ = q_j(N+1) - q_j(N) \qquad (14)$$

$$f_j^- = q_j(N) - q_j(N-1) \qquad (15)$$

$$f_j^0 = \frac{1}{2}[q_j(N+1) - q_j(N-1)] \qquad (16)$$

where f_j^+, f_j^- and f_j^0 are nucleophilic, electrophilic and free radical on the reference molecule, respectively. In these equations, q_j is the atomic charge

at the jth atomic site for the neutral (N), anionic (N + 1) or cationic (N − 1) chemical species. Previously Morell et al. [65] anticipated a dual descriptor ($\Delta f(r)$), that is the alteration among the electrophilic and nucleophilic Fukui function which can be represented according to the following equation:

$$\Delta f(r) = f_j^+ - f_j^- \qquad (17)$$

If the $\Delta f(r) > 0$, then the site might be ideal for a nucleophilic attack, however if $\Delta f(r) < 0$, then the site is favorite for an electrophilic attack. The values of calculated Fukui functions f_j^+, f_j^- and f_j^0) and $\Delta f(r)$ have been given in Table 4. Here, the $\Delta f(r)$ gives a clear difference between nucleophilic and electrophilic attack at a specific position with positive or negative sign. The positive value suggests a nucleophilic attack while the negative one, electrophilic attack. It is expected that Cl (1), N (3) and N (4) sites would be favorable for the nucleophilic attack (i.e. $\Delta f(r) > 0$), while O (2) position for the electrophilic attack (i.e. $\Delta f(r) < 0$) in 1. In 2, nucleophilic sites are Br (1), N (3) and N (5) (i.e. $\Delta f(r) > 0$) while electrophilic sites O (2) and H (4) (i.e. $\Delta f(r) < 0$). In 3, S (27) site would be favorite for nucleophilic attack (i.e. $\Delta f(r) > 0$), whereas O (1), N (2) and N (4) for electrophilic attack (i.e. $\Delta f(r) < 0$). But the electrophilic and nucleophilic attack performance of the molecule during reaction depends on the local behavior.

3.6. Charge transport parameters

The IP and EA highlight the charge transfer performance; lower IP shows that the compound could be a good hole transporter while higher EA leads to electron transport. The IPa/v and EAa/v have been shown in Table 5. The IPa/v of 2 and 3 decrease of 0.20/0.10 eV and 0.13/0.13 eV compared to 1, respectively. The EAa/v of 2 is lower than those of other counterparts. The higher EAv of 3 than of the other compounds (1 and 2) reveals that electron injection ability of this compound would be superior than of the other ones. The reorganization energies of electron λ (e) and reorganization energies of hole λ (h) for hydroquinoline derivatives (in eV) at the B3LYP/6-31G** level are tabulated in Table 5. The

Table 4. The calculated Fukui indices $\mathfrak{f}_j^+$, $\mathfrak{f}_j^-$ and $\mathfrak{f}_j^0$ as well as $\Delta f(r)$ of the studied compounds.

Compound	Atom No.	$\mathfrak{f}_j^-$	$\mathfrak{f}_j^+$	$\mathfrak{f}_j^0$	$\Delta f(r)$
1	Cl (1)	0.005	0.007	0.006	0.002
	O (2)	0.015	0.006	0.010	–0.009
	N (3)	0.006	0.017	0.011	0.011
	N (4)	0.011	0.022	0.016	0.011
2	Br (1)	0.019	0.029	0.024	0.010
	O (2)	0.006	0.005	0.005	–0.001
	N (3)	–0.001	0.001	0.000	0.002
	H (4)	0.014	0.013	0.014	–0.001
	N (5)	–0.001	0.000	–0.001	0.002
3	O (1)	0.017	0.016	0.016	–0.001
	N (2)	0.006	0.003	0.004	–0.003
	H (3)	0.009	0.014	0.011	0.005
	N (4)	0.005	0.001	0.003	–0.004
	S (27)	0.010	0.016	0.013	0.006

computed λ (h) of 3 and 1 are smaller than that of 2 showing that hole transporting capability of these compounds would be higher than that of the latter compound. Additionally, the computed λ (e) of all the derivatives in this study are higher than λ (h), showing that the charge transport behavior might be hole dominant.

The C–O bond length of 1 anion is lengthened of 0.016 Å, while 1 cation is shortened of 0.004 Å compared to the neutral one. The C–Br bond lengths of 2 anion/2 cation are lengthened/shortened of 0.72 Å/0.020 Å compared to the neutral form, respectively. Major lengthening and shortening in 3 anion/3 cation have been found in the C–O and C–S bond lengths, i.e. C–O of 3 anion/3 cation are lengthened/shortened of 0.017 Å/0.002 Å, while C–S of 3 anion/3 cation are lengthened of 0.041 Å/0.006 Å compared to the neutral form, respectively. We found that the geometry relaxation between neutral and anion states is higher than between neutral and cation states causing further polarization in anion states resulting in larger λ (e) values than the λ (h). The maximum geometry relaxation in compound 2 leads to the utmost λ (e) diminishing electron charge transport character.

3.7. Nonlinear optical properties

Recently, the organic materials have provided a good boost in the field of nonlinear optical

Table 5. Vertical and adiabatic ionization potentials (IPv/IPa), vertical and adiabatic electronic affinities (EAv/EAa), hole reorganization energies λ (h), and electron reorganization energies λ (e) of hydroquinoline derivatives (in eV) at the B3LYP/6-31G** level of theory.

Compounds	IPa	EAa	IPv	EAv	λ (h)	λ (e)
1	7.68	0.026	7.81	0.39	0.259	0.554
2	7.48	–0.001	7.71	–0.59	0.521	2.690
3	7.55	0.026	7.68	0.46	0.253	0.453

(NLO) materials designing. The field of designing of NLO-phores is of significant importance due to the possibility of application in several fields including frequency doubling, fast data processing, SHG spectroscopy etc. There are many efforts devoted to obtain NLO materials with required amplitude of NLO response [66]. In this regard, the organic class of materials is considered to be very promising because of their low cost, ease of fabrication as well as large NLO response [67, 68]. In present investigation, the compounds 1 – 3 have electronic transitions involving intramolecular charge redistribution as illustrated by the patterns of their frontier molecular orbitals in ground state, which indicate their possible potential for efficient NLO phores. To check the possibility of these compounds for their potential applications as NLO materials, we have calculated their

molecular electronic static first hyperpolarizability (β_{tot}). The first hyperpolarizability and its components for all compounds 1 – 3 were calculated using finite field (FF) approach. The B3LYP/6-31G** level of theory combined with finite field (FF) approach have been used to calculate the first hyperpolarizability (β_{tot}) of the title compounds. The FF method, which has originally been developed by Kurtz et al. [69] is usually applied to calculate the first hyperpolarizability of organic molecules because it provides very reliable results, consistent with experiments [68, 70] and other computational approaches [71]. A static electric field (F) is applied in FF approach and the energy (E) of a molecule is given by following equation:

$$E = E^{(0)} - \mu_1 F_1 - \frac{1}{2}\alpha_{ij}F_iF_j - \frac{1}{6}\beta_{ijk}F_iF_jF_k$$
$$- \frac{1}{24}\gamma_{ijkl}F_iF_jF_kF_l - \dots \quad (18)$$

In the absence of an electric field, the total energy of molecule is represented by $E^{(0)}$, μ is the dipole moment, α is the polarizability, β and γ are the first and second hyperpolarizabilities, respectively, while x, y and z label the i, j and k components, respectively. It can be seen from above equation that differentiating E with respect to F gives the μ, α, β, and γ values. Here, β, and γ values represent the origin of second-order (χ^2) and third-order (χ^3) nonlinear optical (NLO) susceptibilities, respectively. In our present investigation, we have calculated the molecular first hyperpolarizability. The magnitude of first static hyperpolarizability (β_{tot}) can be calculated using following equations:

$$\beta_{tot} = \left(\beta_x^2 + \beta_y^2 + \beta_z^2\right)^{\frac{1}{2}} \quad (19)$$

where

$$\beta_x = \beta_{xxx} + \beta_{xyy} + \beta_{xzz} \quad (20)$$

$$\beta_y = \beta_{yyy} + \beta_{xxy} + \beta_{yzz} \quad (21)$$

$$\beta_z = \beta_{zzz} + \beta_{xxz} + \beta_{yyz} \quad (22)$$

The first static hyperpolarizability (β) that is a third rank tensor can be described by a $3 \times 3 \times 3$ matrix. According to Kleinman symmetry ($\beta_{xyy} = \beta_{yxy} = \beta_{yyx}$, $\beta_{yyz} = \beta_{yzy} = \beta_{zyy}$,... likewise other permutations also take same value), the 27 components of the 3D matrix can be reduced to 10 components as given in Table 6.

In Table 6, the values of hyperpolarizability (β_{tot}) calculated at B3LYP/6-31G* level of theory are collected. All the above reported compounds have non-zero value of their β_{tot} amplitudes, which are 302, 86 and 328 a. u. for compounds 1, 2 and 3, respectively. The non-zero value of β_{tot} shows that the title molecules possess different amplitudes of microscopic first static hyperpolarizability. A comparison with static hyperpolarizability of urea molecule (a prototype NLO molecule used as reference in experimental calculation of first hyperpolarizability), calculated at the same level of theory shows that compounds 1, 2 and 3 have ∼7 times, 2 times and 8 times larger amplitudes of their β_{tot} values as compared to that of urea molecules (43 a.u.). Thus, the above comparison highlights the importance of the designed compounds to be used as efficient NLO-phores.

4. Conclusions

In the framework of our present quantum chemical study of selected compounds 1, 2 and 3, the following conclusions can be drawn as:

1. The ground state geometrical parameters calculated at B3LYP/6-31G** levels of theory are in good agreement with the experimental crystal structural parameters.

2. The comprehensive intra-molecular charge transport has been observed in compound 2. It is expected that higher E_g of all the studied compounds could cause them to be thermodynamically stable.

3. The deep valence band is defined mostly by the s orbitals while upper valence bands are due to the p orbitals. In lower conduction bands, the peaks are due to the p orbitals except Br in 2 in which s-orbital is involved.

Table 6. Calculated values of first hyperpolarizability (β) along their individual tensor components for compounds 1 – 3 at B3LYP/6-31G* level of theory.

1		2		3	
Component	a.u.	Component	a.u.	Component	a.u.
β_{xxx}	223	β_{xxx}	1	β_{xxx}	128
β_{xxy}	–57	β_{xxy}	–41	β_{xxy}	10
β_{xyy}	–23	β_{xyy}	23	β_{xyy}	14
β_{yyy}	20	β_{yyy}	117	β_{yyy}	10
β_{xxz}	–314	β_{xxz}	–1	β_{xxz}	383
β_{xyz}	39	β_{xyz}	–19	β_{xyz}	24
β_{yyz}	–23	β_{yyz}	95	β_{yyz}	–35
β_{xzz}	12	β_{xzz}	–4	β_{xzz}	154
β_{yzz}	22	β_{yzz}	–25	β_{yzz}	21
β_{zzz}	123	β_{zzz}	–160	β_{zzz}	–212
β_{tot}	302	β_{tot}	86	β_{tot}	328
β_{tot} (urea)[a]	43	β_{tot} (urea)[a]	43	β_{tot} (urea)[a]	43

For β, 1 a.u. = 0.008629 $\times$ 10^{-30} esu, [a]calculated in present study at the same B3LYP/6-31G* level of theory.

4. In 1, negative potential region is on the Cl atom, revealing that it would be favorable for electrophilic attack. In contrast, the N atom exhibits the positive electrostatic potential regions being favorable for the electrophilic attack.

5. The smaller η and χ values of 2 than of other derivatives suggest that aforementioned compound would be more stable with lower chemical activity.

6. It is expected that N (3) and N (4) sites would be favorable for the nucleophilic attack while O (2) position for the electrophilic attack in 1. In 2, nucleophilic sites are Br (1), N (3) and N (5) while electrophilic sites are O (2) and H (4). In 3, H (3) and S (27) sites would be preferred for nucleophilic attack whereas O (1), N (2) and N (4) for electrophilic one.

7. The smaller hole reorganization energy values as compared to the electron values show that all these compounds might participate in hole transport. The smaller hole reorganization energy of 1 and 3 than that of 2 implies that these compounds would be better hole transport materials than the latter one.

8. The higher geometry relaxation between neutral and anion states than neutral and cation states triggering polarization in anion states result in the higher λ (e) values than the λ (h).

Acknowledgements

References

[1] MASSARANI E., NARDI D., POZZI R., DEGEN L., MAGISTRETTI M.J., *J. Med. Chem.,* 13 (1970), 380.

[2] SEGAL I., ZABLOTSKAYA A., LUKEVICS E., *Chem. Heterocycl. Compd.,* 41 (2005), 613.

[3] ABDEL-GAWAD S.M., EL-GABY M.S.A., HEIBA H.I., ALY H.M., GHORAB M.M., *J. Chin. Chem. Soc.,* 52 (2005), 1227.

[4] LEVINE H., 3RD, DING Q., WALKER J.A., VOSS R.S., AUGELLI-SZAFRAN C.E., *Neurosci. Lett.,* 465 (2009), 99.

[5] ADHIKARI A., KALLURAYA B., SUJITH K.V., GOUTHAMCHANDRA, MAHMOOD R., *Saudi Pharmaceutical J.,* 20 (2012), 75.

[6] HUIGUO LAI G.S.P., RADHAKRISHNAN PADMANABHAN, *Antiviral Res.,* 97 (2013), 74.

[7] IRFAN A., CUI R., ZHANG J., *Chem. Phys.,* 358 (2009), 25.

[8] IRFAN A., CUI R., ZHANG J., NADEEM M., *Aust. J. Chem.,* 63 (2010), 1283.

[9] PRACHAYASITTIKUL V P.S., RUCHIRAWAT S, PRACHAYASITTIKUL V, *Drug Des. Dev. Ther.,* 7 (2013), 1157.

[10] CHUPAKHINA T.A., KATSEV A.M., KUR'YANOV V.O., *USS. J. Bioorg. Chem.,* 38 (2012), 422.

[11] BEN KHALIFA M., VAUFREY D., TARDY J., *Org. Electron.,* 5 (2004), 187.

[12] LENZI O., COLOTTA V., CATARZI D., VARANO F., SQUARCIALUPI L., FILACCHIONI G., VARANI K., VINCENZI F., BOREA P.A., BEN D.D., LAMBERTUCCI C., CRISTALLI G., *Biorg. Med. Chem.,* 19 (2011), 3757.

[13] SHEN A.-Y., WU S.-N., CHIU C.-T., *J. Pharm. Pharmacol.,* 51 (1999), 543.

[14] BAHGAT K., RAGHEB A.G., *Central European J. Chem.,* 5 (2007), 201.

[15] TENG Y.H.K., SU Z.M., LIAO Y., YANG S.Y., WANG R.S., *Theor. Chem. Acc.,* 117 (2007), 1.

[16] RAMS-BARON M.D., MROZEK-WILCZKIEWICZ A., KORZEC M., CIESLIK W., SPACZYŃSKA E., BARTCZAK P., RATUSZNA A., POLANSKI J., MUSIOL R., *PLoS One,* 10 (2015), e0131210.

[17] ASIRI A.M., AL-YOUBI A.O., FAIDALLAH H.M., BADAHDAH K.O., NG S.W., *Acta Crystallogr. Sect. E,* 67 (2011), o2596.

[18] ASIRI A.M., FAIDALLAH H.M., NG S.W., TIEKINK E.R.T., *Acta Crystallogr. Sect. E,* 68 (2012), o2376.

[19] ASIRI A.M., FAIDALLAH H.M., SAQER A.A.A., NG S.W., TIEKINK E.R.T., *Acta Crystallogr. Sect. E,* 68 (2012), o2291.

[20] LI Y., ZOU L.-Y., REN A.-M., FENG J.-K., *Comp. Theor. Chem.,* 981 (2012), 14.

[21] CHAUDHRY A.R., AHMED R., IRFAN A., MUHAMMAD S., SHAARI A., AL-SEHEMI A.G., *Comp. Theor. Chem.,* 1045 (2014), 123.

[22] IRFAN A., AL-SEHEMI A.G., AL-ASSIRI M.S., *Comp. Theor. Chem.,* 1031 (2014), 76.

[23] ZGIERSKI M.Z., LIM E.C., FUJIWARA T., *Comp. Theor. Chem.,* 1036 (2014), 1.

[24] MAHMOOD A., TAHIR M.H., IRFAN A., AL-SEHEMI A.G., AL-ASSIRI M., *Comp. Theor. Chem.,* 1066 (2015), 94.

[25] IRFAN A., ABDULLAH G., ABDULLAH M.A., *J. Theor. Comput. Chem.,* 11 (2012), 631.

[26] IRFAN A., *J. Theor. Comput. Chem.,* 13 (2014), 1450013.

[27] A. IRFAN S., MUHAMMAD, A.G. AL-SEHEMI, M.S. AL-ASSIRI, A. KALAM, A.R. CHAUDHRY, *J Theor Comput Chem,* 14 (2015), 1550027.

[28] MUHAMMAD S., IRFAN A., AL-SEHEMI A.G., AL-ASSIRI M.S., KALAM A., CHAUDHRY A.R., *J. Theor. Comput. Chem.,* 14 (2015), 1550029.

[29] BECKE A.D., *J. Chem. Phys.,* 98 (1993), 5648.

[30] SALVATORI P., AMAT A., PASTORE M., VITILLARO G., SUDHAKAR K., GIRIBABU L., SOUJANYA Y., ANGELIS DE F., *Comp. Theor. Chem.,* 1030 (2014), 59.

[31] FU J.-J., DUAN Y.-A., ZHANG J.-Z., GUO M.-S., LIAO Y., *Comp. Theor. Chem.,* 1045 (2014), 145.

[32] IRFAN A., KALAM A., CHAUDHRY A.R., AL-SEHEMI A.G., MUHAMMAD S., *Optik - Intern. J. Light Elect. Optics,* 132 (2017), 101.

[33] SÁNCHEZ-CARRERA R.S., COROPCEANU V., SILVA DA FILHO D.A., FRIEDLEIN R., OSIKOWICZ W., MURDEY R., SUESS C., SALANECK W.R., BRÉDAS J.-L., *J. Phys. Chem. B,* 110 (2006), 18904.

[34] WONG B.M., CORDARO J.G., *J. Chem. Phys.,* 129 (2008).

[35] MATCZAK P., *Comp. Theor. Chem.,* 983 (2012), 25.

[36] FEREYDUNI E., VESSALLY E., YAAGHUBI E., SUNDARAGANESAN N., *Spectrochimica Acta A,* 81 (2011), 64.

[37] IRFAN A., AL-SEHEMI A.G., CHAUDHRY A.R., MUHAMMAD S., *Optik - Intern. J. Light Elect. Optics,* 138 (2017), 349.

[38] STRASSNER T., TAIGE M.A., *J. chem. theor. comput.,* 1 (2005), 848.

[39] SOUSA S.F., FERNANDES P.A., RAMOS M.J., *J. Phys. Chem. A,* 111 (2007), 10439.

[40] MUSA K.A.K., ERIKSSON L.A., *J. Phys. Chem. A,* 112 (2008), 10921.

[41] GUILLAUMONT D., NAKAMURA S., *Dyes Pigm.,* 46 (2000), 85.

[42] AL-SEHEMI A., AL-MELFI M., IRFAN A., *Struct. Chem.,* 24 (2013), 499.

[43] IRFAN A., AL-SEHEMI A., *J. Mol. Model.,* 18 (2012), 4893.

[44] IRFAN A., HINA N., AL-SEHEMI A., ASIRI A., *J. Mol. Model.,* 18 (2012), 4199.

[45] IRFAN A., AL-SEHEMI A.G., KALAM A., *J. Mol. Struct.,* 1049 (2013), 198.

[46] AL-SEHEMI A.G., IRFAN A., AL-MELFI M.A.M., *Spectrochim. Acta A,* 145 (2015), 40.

[47] IRFAN A., JIN R., AL-SEHEMI A.G., ASIRI A.M., *Spectrochim. Acta A,* 110 (2013), 60.

[48] AL-SEHEMI A.G., IRFAN A., FOUDA A.M., *Spectrochim. Acta A,* 111 (2013), 223.

[49] TRUJILLO C., LAMSABHI A.M., MÓ O., YÁÑEZ M., SALPIN J.-Y., *Int. J. Mass Spectrom.,* 306 (2011), 27.

[50] BEGTRUP M., BALLE T., CLARAMUNT R.M.A., SANZ D., JIMÉNEZ J.A., MÓ O., YÁÑEZ M., ELGUERO J., *J. Mol. Struct. (TheoChem),* 453 (1998), 255.

[51] CORRAL I., MÓ O., YÁÑEZ M., *Int. J. Mass spectrom.,* 255 – 256 (2006), 20.

[52] ZHANG C., LIANG W., CHEN H., CHEN Y., WEI Z., WU Y., *J. Mol. Struct. (TheoChem),* 862 (2008), 98.

[53] IRFAN A., AL-SEHEMI A.G., MUHAMMAD S., CHAUDHRY A.R., KALAM A., SHKIR M., AL-SALAMI A.E., ASIRI A.M., *J. Saudi. Chem. Soc.,* 20 (2016), 680.

[54] IRFAN A., AL-SEHEMI A.G., MUHAMMAD S., CHAUDHRY A.R., AL-ASSIRI M.S., JIN R., KALAM A., SHKIR M., ASIRI A.M., *Comptes Rendus Chim.,* 18 (2015), 1289.

[55] SCALMANI G., FRISCH M.J., MENNUCCI B., TOMASI J., CAMMI R., BARONE V., *J. Chem. Phys.,* 124 (2006), 094107.

[56] MARCUS R.A., *Rev. Mod. Phys.,* 65 (1993), 599.

[57] BRÉDAS J.L., CALBERT J.P., DA SILVA FILHO D.A., CORNIL J., *Proc. Natl. Acad. Sci.,* 99 (2002), 5804.

[58] GRUHN N.E., DA SILVA FILHO D.A., BILL T.G., MALAGOLI M., COROPCEANU V., KAHN A., BRÉDAS J.-L., *J. Am. Chem. Soc.,* 124 (2002), 7918.

[59] REIMERS J.R., *J. Chem. Phys.,* 115 (2001), 9103.

[60] M. J. FRISCH G.W.T., SCHLEGEL H.B., SCUSERIA G.E., ROBB M.A., CHEESEMAN J.R., SCALMANI G., BARONE V., MENNUCCI B., PETERSSON G.A., NAKATSUJI H., CARICATO M., LI X., HRATCHIAN H.P., IZMAYLOV A.F., BLOINO J., ZHENG G., SON- NENBERG J.L., HADA M., EHARA M., TOYOTA K., FUKUDA R., HASEGAWA J., ISHIDA M., NAKAJIMA T., HONDA Y., KITAO O., NAKAI H., VREVEN T., MONTGOMERY J.A. JR., PERALTA J.E., OGLIARO F., BEARPARK M., HEYD J.J., BROTHERS E., KUDIN K.N., STAROVEROV V.N., KOBAYASHI R., NOR- MAND J., RAGHAVACHARI K., RENDELL A., BURANT J.C., IYENGAR S.S., TOMASI J., COSSI M., REGA N., MILLAM J.M., KLENE M., KNOX J.E., CROSS J.B., BAKKEN V., ADAMO C., JARAMILLO J., GOMPERTS R., STRATMANN R.E., YAZYEV O., AUSTIN A.J., CAMMI R., POMELLI C., OCHTERSKI J.W., MAR- TIN R.L., MOROKUMA K., ZAKRZEWSKI V.G., VOTH G.A., SALVADOR P., DANNENBERG J.J., DAPPRICH S., DANIELS A.D., FARKAS Ö., FORESMAN J.B., OR- TIZ J.V., CIOSLOWSKI J., FOX D.J., in: *Gaussian 09*, Revision A. 01,, Gaussian Inc., Wallingford, CT, 2009.

[61] CLARK S.J., SEGALL M.D., PICKARD C.J., HASNIP P.J., PROBERT M.I., REFSON K., PAYNE M.C., *Z. Kristallogr. Cryst. Mater.,* 220 (2005), 567.

[62] MATERIALSSTUDIO, (2013).

[63] PERDEW J.P., WANG Y., *Phys. Rev. B,* 45 (1992), 13244.

[64] AYERS P.W., PARR R.G., *J. Am. Chem. Soc.,* 122 (2000), 2010.

[65] MORELL C., GRAND A., TORO-LABBÉ A., *J. Phys. Chem. A,* 109 (2005), 205.

[66] LEVINE B.F., BETHEA C.G., *J. Chem. Phys.,* 63 (1975), 2666.

[67] BADAN J., HIERLE R., PERIGAUD A., ZYSS J., WILLIAMS D., *NLO properties of organic molecules and polymeric materials*, in: *American Chemical Society Symposium Series*, American Chemical Society Wash- ington DC, 1993.

[68] MUHAMMAD S., IRFAN A., SHKIR M., CHAUDHRY A.R., KALAM A., ALFAIFY S., AL-SEHEMI A.G., AL-SALAMI A., YAHIA I., XU H.L., *J. Comput. Chem.,* 36 (2015), 118.

[69] KURTZ H.A., STEWART J.J.P., DIETER K.M., *J. Com- put. Chem.,* 11 (1990), 82.

[70] NAGAPANDISELVI P., BABY C., GOPALAKRISHNAN R., *J. Mol. Struct.,* 1056 – 1057 (2014), 110.

[71] DEHU C., MEYERS F., BREDAS J.L., *J. Am. Chem. Soc.,* 115 (1993), 6198.